The auxiliary glutamate receptor subunit dSol-1 promotes presynaptic neurotransmitter release and homeostatic potentiation

Beril Kiragasi[a,1], Pragya Goel[a,1], Sarah Perry[a], Yifu Han[a], Xiling Li[a], and Dion Dickman[a,2]

[a]Department of Neurobiology, University of Southern California, Los Angeles, CA 90089

Edited by Ehud Y. Isacoff, University of California, Berkeley, CA, and approved August 27, 2020 (received for review September 9, 2019)

Presynaptic glutamate receptors (GluRs) modulate neurotransmitter release and are physiological targets for regulation during various forms of plasticity. Although much is known about the auxiliary subunits associated with postsynaptic GluRs, far less is understood about presynaptic auxiliary GluR subunits and their functions. At the *Drosophila* neuromuscular junction, a presynaptic GluR, *DKaiR1D*, localizes near active zones and operates as an autoreceptor to tune baseline transmission and enhance presynaptic neurotransmitter release in response to diminished postsynaptic GluR functionality, a process referred to as presynaptic homeostatic potentiation (PHP). Here, we identify an auxiliary subunit that collaborates with DKaiR1D to promote these synaptic functions. This subunit, dSol-1, is the homolog of the *Caenorhabditis elegans* CUB (Complement C1r/C1s, Uegf, Bmp1) domain protein Sol-1. We find that *dSol-1* functions in neurons to facilitate baseline neurotransmission and to enable PHP expression, properties shared with *DKaiR1D*. Intriguingly, presynaptic overexpression of *dSol-1* is sufficient to enhance neurotransmitter release through a *DKaiR1D*-dependent mechanism. Furthermore, *dSol-1* is necessary to rapidly increase the abundance of DKaiR1D receptors near active zones during homeostatic signaling. Together with recent work showing the CUB domain protein Neto2 is necessary for the homeostatic modulation of postsynaptic GluRs in mammals, our data demonstrate that dSol-1 is required for the homeostatic regulation of presynaptic GluRs. Thus, we propose that CUB domain proteins are fundamental homeostatic modulators of GluRs on both sides of the synapse.

glutamate receptor | auxiliary subunit | *Drosophila* | homeostatic plasticity | synapse

Synaptic strength is dynamically tuned during both Hebbian and homeostatic forms of plasticity. One major mechanism that achieves this modulation targets the abundance, localization, and/or functionality of ionotropic glutamate receptors (GluRs). For instance, the expression of long-term potentiation and depression requires bidirectional changes in the abundance of postsynaptic α-amino-3-hydroxy-5-methyl-4-isoxazolepropionic acid (AMPA) receptors to adjust synaptic strength (1–3). Furthermore, some forms of homeostatic plasticity also tune the abundance of *N*-methyl-D-aspartate (NMDA), AMPA, and kainate receptors at postsynaptic densities to stabilize neuronal activity (4–6). Auxiliary subunits associated with GluRs are key factors that control GluR trafficking and dynamics during plasticity, where transmembrane AMPA receptor regulatory protein (TARP), Cornichon, and Neto subunits orchestrate AMPA and kainate receptor function and plasticity (7–9). Although much is known about the GluR subtypes and associated auxiliary subunits that regulate GluR trafficking, abundance, and functionality at postsynaptic densities during both Hebbian and homeostatic plasticity, far less is understood about these mechanisms at presynaptic release sites.

Presynaptic autoreceptors have emerged as important regulators of neurotransmitter release at glutamatergic synapses. For example, presynaptic kainate receptors are present in hippocampal mossy fibers, where autocrine feedback facilitates neurotransmission during trains of activity (10–12). In addition, presynaptic NMDA receptors in the hippocampus mediate presynaptic inhibition in response to excess glutamate release as well as presynaptic facilitation following the induction of long-term potentiation (13). Furthermore, presynaptic metabotropic receptors play critical roles in various forms of plasticity and can bidirectionally tune presynaptic neurotransmitter release (14–16). Finally, ionotropic neurotransmitter receptors at presynaptic terminals can modulate release at neuromuscular junctions (NMJs) in *Caenorhabditis elegans* and *Drosophila* (17, 18). While it is now clear that presynaptic autoreceptors are important bidirectional modulators of neurotransmitter release, how the levels, activity, and localization of these receptors are controlled to establish baseline function, and to what extent they are further modified during plasticity, remains unclear.

A kainate-type ionotropic GluR, *DKaiR1D*, was previously shown to be necessary at the *Drosophila* NMJ for the expression of presynaptic homeostatic potentiation (PHP) (17). PHP is a fundamental form of synaptic plasticity in which pharmacological and genetic challenges that diminish postsynaptic neurotransmitter receptor functionality trigger a transsynaptic retrograde signal that enhances presynaptic neurotransmitter release to precisely compensate for reduced postsynaptic excitability (19, 20). PHP has been observed at NMJs of *Drosophila* (21), rodents (22–24), and humans (25, 26) and was recently demonstrated to be rapidly expressed in the mammalian central nervous system (27). *DKaiR1D* was identified in a forward genetic screen to be required for the rapid expression of PHP at the fly NMJ (17). DKaiR1D receptors form homomers that are permeable to both sodium and calcium (28), localized near presynaptic release sites, and proposed to homeostatically regulate presynaptic voltage following autocrine activation by glutamate (17). This DKaiR1D-dependent

Significance

Physiological signals that modulate glutamate receptor trafficking and function remain enigmatic. Here, we identify the auxiliary glutamate receptor subunit *dSol-1* to be necessary for the homeostatic control of presynaptic neurotransmitter release at the *Drosophila* neuromuscular junction. *dSol-1* promotes the accumulation of kainate receptors at presynaptic terminals to enable the synapse-specific expression of homeostatic plasticity.

Author contributions: B.K., P.G., and D.D. designed research; B.K., P.G., S.P., and X.L. performed research; Y.H. contributed new reagents/analytic tools; B.K., P.G., and S.P. analyzed data; and P.G. and D.D. wrote the paper.

The authors declare no competing interest.

This article is a PNAS Direct Submission.

[1]B.K. and P.G. contributed equally to this work.

[2]To whom correspondence may be addressed. Email: dickman@usc.edu.

This article contains supporting information online at https://www.pnas.org/lookup/suppl/doi:10.1073/pnas.1915464117/-/DCSupplemental.

First published September 24, 2020.

enhancement in neurotransmitter output implies a rapid modulation in the abundance, functionality, and/or localization of these receptors must occur in the course of PHP induction. This regulation could, in principle, be achieved through interactions with auxiliary GluR subunits (29, 30). However, the precise mechanisms that control DKaiR1D and enable robust and stable neurotransmission at baseline and during plasticity, and whether auxiliary factors are involved, are unknown.

We have performed a candidate screen of *Drosophila* GluR modulators and auxiliary subunits to identify potential functions in PHP expression. This effort has discovered an uncharacterized auxiliary GluR subunit that functions in neurons to promote neurotransmitter release and enable homeostatic potentiation. This factor, a homolog of the *C. elegans* auxiliary GluR subunit *Sol-1* (31), contains multiple CUB domains and is structurally similar to the Neto/Sol-2 family of auxiliary GluR subunits (6, 32–34). *dSol-1* mutants essentially phenocopy *DKaiR1D* mutants in neurotransmission and PHP. Further experiments demonstrate that *dSol-1* functions to homeostatically modulate presynaptic glutamate release by promoting the rapid accumulation of DKaiR1D receptors near active zones. Together, these data indicate that the interactions between CUB domain auxiliary subunits and their associated GluRs are fundamental physiological targets of homeostatic signaling.

Results

A Screen of *Drosophila* GluR Modulators and Putative Auxiliary Subunits Identifies *dSol-1* to Be Necessary for PHP Expression. The kainate receptor DKaiR1D functions at presynaptic terminals of the *Drosophila* NMJ to homeostatically increase presynaptic neurotransmitter release following pharmacological attenuation of postsynaptic GluRs using philanthotoxin-433 (PhTx; schematized in Fig. 1 *A* and *B*) (17). Auxiliary subunits that associate with AMPA and kainate GluR subtypes in rodents and worms have been identified (7, 35, 36). In *Drosophila*, the homolog of *neto*/*sol-2* is highly expressed in muscle and functions with postsynaptic GluRs at the NMJ (34, 37). We established a candidate list of *Drosophila* genes that are homologs of auxiliary GluR subunits in other systems or that modulate GluR levels in flies to screen for roles in PHP at the NMJ.

We first obtained mutations in three genes that regulate postsynaptic GluR levels at the *Drosophila* NMJ: *coracle* (38), *diablo*/*henji* (39), and *calpain A* (40) (Fig. 1*C* and *SI Appendix*, Table S1). In addition, we identified three homologs of auxiliary GluR subunits that have not been characterized in *Drosophila*: *cornichon*, *stargazin-like*, and *CG34402*/*dSol-1* (Fig. 1*E* and *SI Appendix*, Table S1). We obtained mutations or RNA interference (RNAi) lines targeting each of these genes (*SI Appendix*, Table S1) and assessed PHP expression following PhTx application. Baseline transmission was consistent with previously published data for mutations in these genes (*SI Appendix*, Table S1). Following application of PhTx to the NMJ of these mutants, miniature excitatory postsynaptic potential (mEPSP) amplitude was reduced by ∼50%, as expected (Fig. 1 *D* and *F*). A homeostatic increase in presynaptic neurotransmitter release (quantal content) was robustly expressed in mutations targeting *coracle*, *diablo*, *calpain A*, *cornichon*, and *stargazin-like* (Fig. 1 *D* and *E* and *SI Appendix*, Table S1). However, while mEPSP amplitude was reduced in *CG34402* mutants after PhTx application, no increase in quantal content was observed, demonstrating a block in PHP expression (Fig. 1*F*). The allele of *CG34402* we screened (*MI14035*) contains a MiMIC (Minos-mediated integration cassette) transposon insertion into the second intronic region, predicted to generate a premature stop codon before the first CUB domain. PHP was blocked in this allele when homozygous and in trans with a deficiency (Fig. 1*F* and *SI Appendix*, Table S2). Thus, of all candidate mutations screened, PHP failed to be expressed in a single mutation targeting *CG34402*.

CG34402 encodes a protein of orthologous homology to Sol-1, an auxiliary GluR subunit previously identified and characterized in *C. elegans* (31). We therefore named this gene *dSol-1*. *dSol-1* encodes a protein with a high degree of structural similarity to *C. elegans* Sol-1, each containing four extracellular CUB domains and a single transmembrane domain (Fig. 2*A*) (31, 41, 42). *Sol-1*/*dSol-1* shares structural homology with the *Sol-2*/*Neto* family of auxiliary GluR subunits, which contains two extracellular CUB domains, a single transmembrane domain, and an additional LDL (low-density lipoprotein) domain (Fig. 2*A*). In *Drosophila*, two isoforms of *neto* are expressed, *neto-α* and *neto-β*, which differ in the intracellular C-terminal region (Fig. 2*A*). *Sol-1* and *dSol-1* have both been characterized in heterologous cells, where each can regulate the desensitization kinetics of the *C. elegans* AMPA-type GluR GLR1 (42). *dSol-1* has not been previously studied in *Drosophila*, so we generated independent null mutations in *dSol-1* using CRISPR-Cas9 gene editing. A single-guide RNA (sgRNA) was targeted to the first exon of the *dSol-1* open reading frame (ORF), which generated several independent indels (*Experimental Procedures* and Fig. 2*A*). We chose two alleles that were predicted to lead to early stop codons, truncating the protein before the first CUB domain, which we named $dSol\text{-}1^{bk1}$ *and* $dSol\text{-}1^{bk2}$ (Fig. 2*A*). We characterized baseline synaptic function in these *dSol-1* mutant alleles. Although we found no significant change in miniature excitatory postsynaptic current (mEPSC) amplitude, baseline EPSC amplitudes were significantly reduced in *dSol-1* mutants (Fig. 2 *B* and *D* and *SI Appendix*, Table S2). This suggests a role for *dSol-1* in promoting basal presynaptic glutamate release, without any obvious roles in regulating postsynaptic sensitivity to glutamate.

Next, we assessed PHP expression in the *dSol-1* mutant alleles. Following acute inhibition of postsynaptic GluRs by PhTx application, mEPSP values were reduced, as expected, while EPSP values were similarly reduced compared with baseline (Fig. 2 *B* and *C* and *SI Appendix*, Table S2), demonstrating a failure to homeostatically increase presynaptic release (Fig. 2 *B* and *C*). Similar results were observed in both *dSol-1* alleles when homozygous and in trans to a deficiency that removes the entire *dSol-1* locus (Fig. 2 *B* and *C*). We further assayed PHP expression in these genotypes using a two-electrode voltage-clamp configuration (TEVC), and found similar results to current clamp (Fig. 2 *D* and *E* and *SI Appendix*, Table S2). Thus, *dSol-1* promotes baseline neurotransmitter release and is essential for the rapid homeostatic potentiation of presynaptic release following GluR perturbation at the NMJ.

***dSol-1* Functions in Neurons to Promote Baseline Neurotransmission and PHP.** Auxiliary GluR subunits in mammals have distinct expression patterns and functions in the central nervous system (7, 29). To determine the expression of *dSol-1*, we cloned a 4-kb region upstream of the *dSol-1* locus and generated a promotor fusion with the Gal4 transcriptional activator. In combination with a green fluorescent protein (GFP) reporter, we observed *dSol-1* expression throughout the larval brain as well as in motor neurons, while no expression was observed in the postsynaptic muscle (Fig. 3*A*). It is important to note that while this promotor fusion is capable of rescuing PHP in *dSol-1* mutants (see below), it is possible that not all *dSol-1* regulatory information was captured in this promotor and the GFP reporter itself does not provide information about the subcellular localization of dSol-1. This neuronal expression of *dSol-1* is distinct from that of *Drosophila neto-β*, which is highly expressed in the larval muscle (34). Together, these data indicate that *dSol-1* is exclusively expressed in the nervous system and is absent from the postsynaptic muscle at the *Drosophila* larval NMJ.

Next, we assessed baseline synaptic transmission in *dSol-1* mutants and determined the synaptic compartment in which *dSol-1* was required to enable PHP expression. Consistent with *dSol-1* not being expressed in muscle, we found no significant

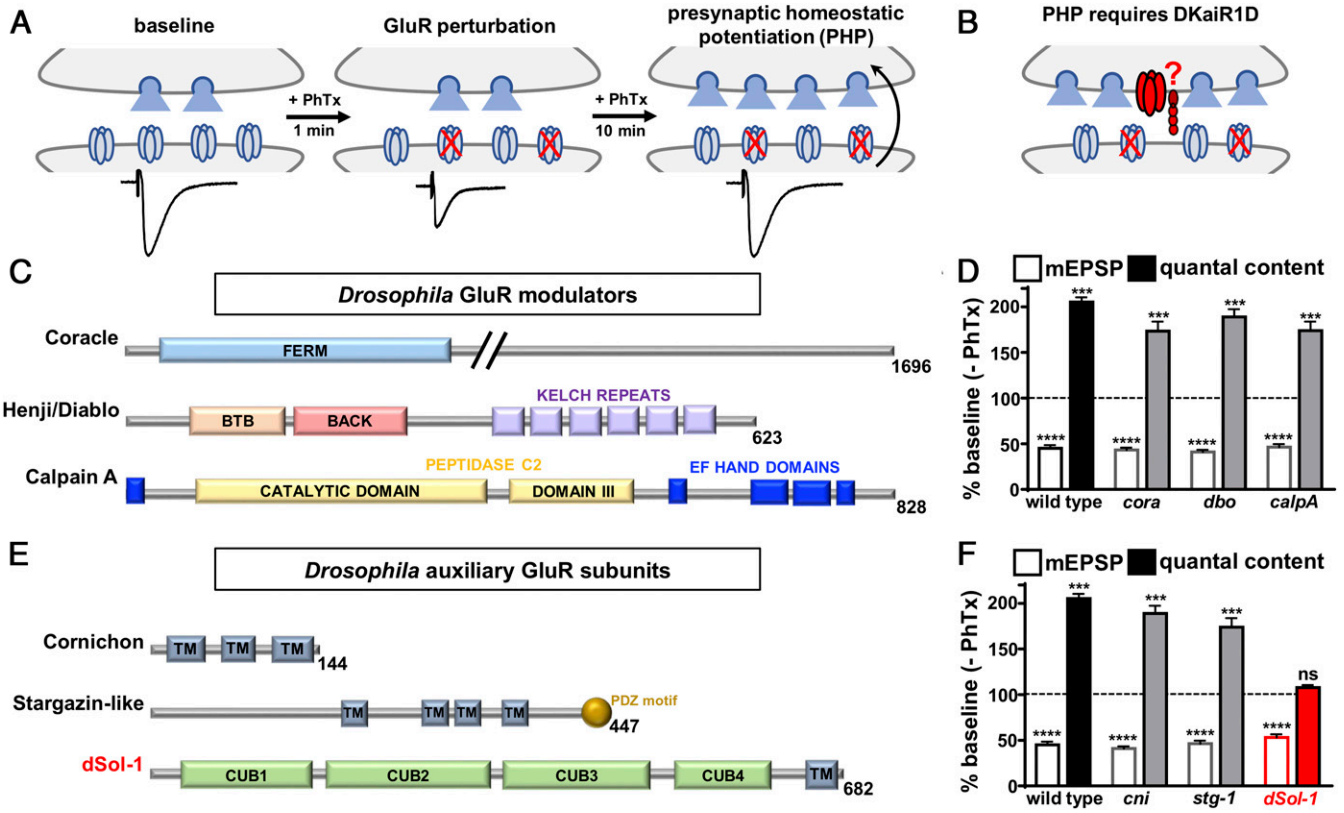

Fig. 1. Candidate screen of GluR modulators and auxiliary subunits identifies dSol-1 to be necessary for PHP. (*A*) Schematic illustrating presynaptic homeostatic potentiation at the *Drosophila* NMJ. Application of the postsynaptic glutamate receptor antagonist philanthotoxin-433 to the larval NMJ initially causes an ~50% reduction in EPSC amplitude. After 10 min, EPSC amplitudes return to baseline values due to a homeostatic enhancement in presynaptic neurotransmitter release (quantal content). (*B*) Schematic showing the presynaptic kainate receptor DKaiR1D (noted in red) functions as an autoreceptor near release sites to enhance neurotransmitter release following PhTx application. The putative auxiliary subunit (also in red) that may function with DKaiR1D is unknown. (*C*) The domain structures of known proteins in *Drosophila* that modulate GluR levels and trafficking are shown. (*D*) Quantification of average mEPSP amplitude and quantal content values in mutations of *coracle* (*cora*: *w;cora*^{MI00820}), *diablo/henji* (*dbo*: *w;dbo*^{8}), and *calpain A* (*calpA*: *w;calpA*^{KG13868}) after PhTx treatment normalized to baseline values (−PhTx). A reduction in mEPSP amplitude but concomitant increase in quantal content demonstrates PHP is expressed in these genotypes. (*E*) The domain structure of putative auxiliary GluR subunits in *Drosophila*. TM, transmembrane domain. (*F*) Quantification of average mEPSP amplitude and quantal content values in putative mutations or RNA interference lines of *cornichon* (*cni*: *OK6-Gal4/+;UAS-cornichon-RNAi/+*), *stargazin-like* (*stg-1*: *stg-1*^{EY06948}), and *dSol-1* (*dSol-1*: *w;dSol-1*^{MI14035}) after PhTx application normalized to baseline values (−PhTx). *dSol-1* mutants fail to increase presynaptic release (quantal content) following PhTx application. Error bars indicate ±SEM. ***$P < 0.001$, ****$P < 0.0001$; ns, not significant. Details of the mutations and RNAi lines screened, their source, and absolute values of electrophysiology data have been summarized in *SI Appendix*, Table S1.

change in mEPSC amplitude nor in the levels of postsynaptic GluRs in *dSol-1* mutants (Fig. 3 *B* and *C* and *SI Appendix*, Fig. S1 *A* and *B*). However, baseline EPSC amplitude was significantly decreased in *dSol-1* mutants, with a concomitant reduction in quantal content (Fig. 3 *B*, *D*, and *E*). In principle, alterations in synaptic growth or number could contribute to this reduced quantal content, but we did not find any significant changes in synaptic growth or active zone density in *dSol-1* mutants (*SI Appendix*, Fig. S1 *C–F*). Importantly, expression of *dSol-1* using either *dSol-1>Gal4* or a motor neuron-specific driver (*OK6-Gal4*) restored synaptic strength to wild-type levels when expressed in *dSol-1* mutant backgrounds (Fig. 3 *B–E* and *SI Appendix*, Table S2), indicating that *dSol-1* functions in motor neurons to promote basal neurotransmitter release. Finally, expression of *dSol-1* in motor neurons, but not in muscle, rescued the block in PHP expression in *dSol-1* mutants (Fig. 3 *B–F*). These results demonstrate that *dSol-1* is expressed in the nervous system, where it functions in motor neurons to promote baseline neurotransmitter release and PHP at the NMJ.

***dSol-1* and *DKaiR1D* Act in the Same Genetic Pathway to Promote Presynaptic Neurotransmitter Release.** It has previously been shown that the presynaptic kainate receptor *DKaiR1D* is also required in motor neurons to promote neurotransmitter release (17). In particular, recording in lowered extracellular Ca^{2+} revealed a reduction in transmission in *DKaiR1D* mutants compared with controls (17). We therefore tested whether *dSol-1* may function in the same genetic pathway as *DKaiR1D* by probing synaptic transmission in *DKaiR1D* or *dSol-1* mutant synapses, as well as in *dSol-1,DKaiR1D* double mutants. Synaptic strength was reduced in *dSol-1* mutants in 0.3 mM Ca^{2+} to levels similar in magnitude to that observed in *DKaiR1D* mutants, and did not change further in *dSol-1,DKaiR1D* double mutants (Fig. 4 *A–D*). These data are consistent with *dSol-1* and *DKaiR1D* functioning together in the same genetic pathway to promote baseline neurotransmission.

The NMDA receptor agonist NMDA was shown to function as an antagonist of DKaiR1D receptors in vitro and in vivo (17, 28). To further test the relationship between *dSol-1* and *DKaiR1D* in basal neurotransmission, we applied NMDA to wild type and *DKaiR1D* and *dSol-1* mutants. First, we confirmed that acute application of NMDA reduces baseline release in wild type at lowered extracellular Ca^{2+} to the same level observed in *DKaiR1D* mutants, with no effect on mEPSCs (Fig. 4 *E–G*). In addition, application of NMDA to *DKaiR1D* mutants had no impact, as expected (Fig. 4 *E–G*). Finally, NMDA application to *dSol-1*

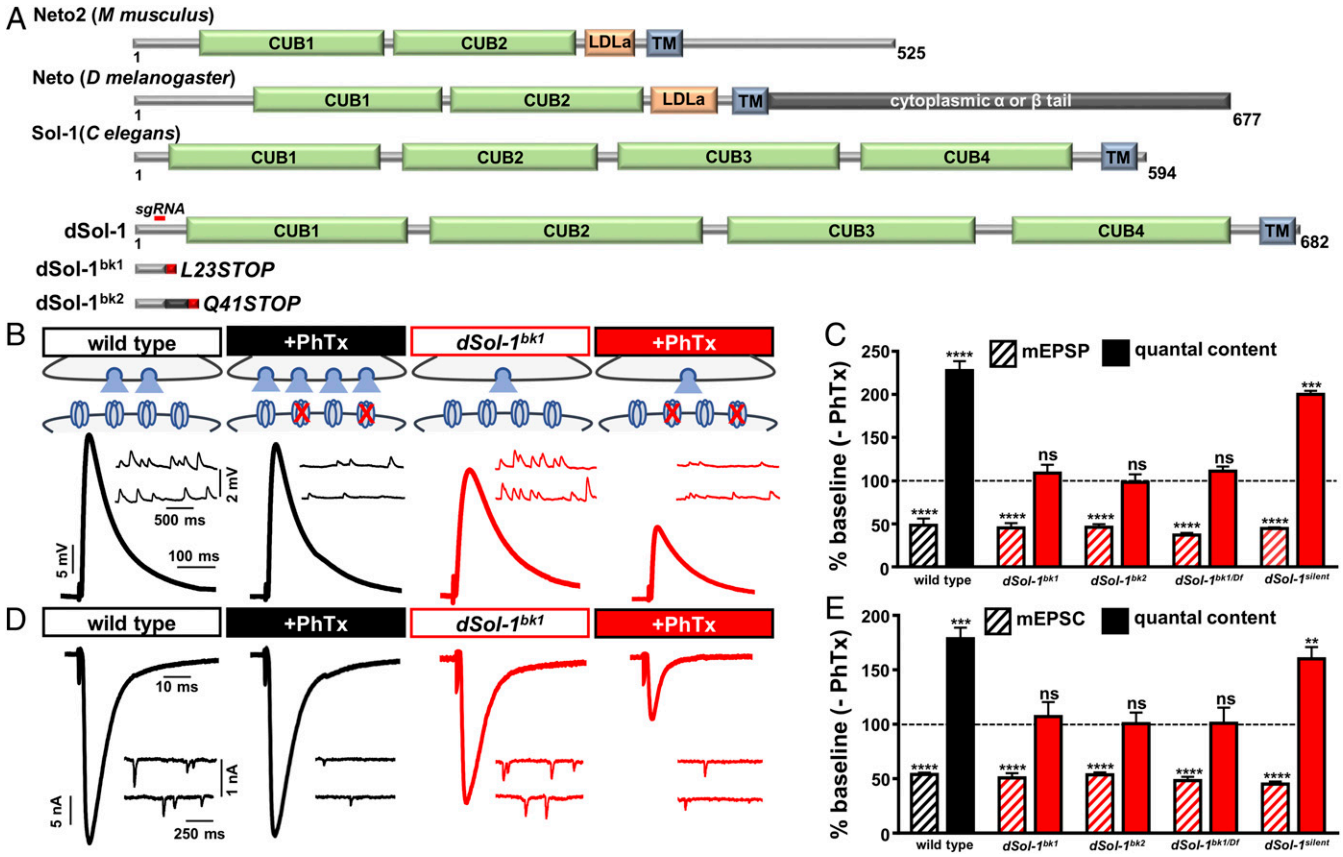

Fig. 2. Auxiliary glutamate receptor subunit *dSol-1* is required for rapid PHP expression. (*A*) Protein structure of Neto2, Neto, Sol-1, and dSol-1 (from the indicated organisms), with the region targeted by the single-guide RNA to generate the *dSol-1*^{bk1} and *dSol-1*^{bk2} mutant alleles and their predicted protein products indicated below. (*B*) Representative mEPSP and EPSP traces in wild type (*w*^{1118}), *dSol-1*^{bk1} (*w;dSol-1*^{bk1}), *dSol-1*^{bk2} (*w;dSol-1*^{bk2}), *dSol-1*$^{bk1/Df}$ [*w;dSol-1*^{bk1}*/Df(3R)Exel7315*], and *dSol-1*^{silent} (*w;dSol-1*^{silent}) at baseline and after PhTx application. While PhTx application reduces mEPSP amplitudes in all genotypes, as expected, EPSP amplitude fails to return to baseline levels in all *dSol-1* mutant alleles and combinations following PhTx application due to a failure to enhance presynaptic neurotransmitter release (quantal content). (*C*) Quantification of mEPSP amplitude and quantal content values in the indicated genotypes following PhTx application relative to baseline (−PhTx). (*D*) Representative mEPSC and EPSC traces in two-electrode voltage-clamp configuration in the indicated genotypes at baseline and after PhTx application. (*E*) Quantification of mEPSC amplitude and quantal content TEVC values in the indicated genotypes and conditions. Error bars indicate ±SEM. $^{**}P < 0.01$, $^{***}P < 0.001$, $^{****}P < 0.0001$; ns, not significant. Absolute values for normalized data are summarized in *SI Appendix*, Table S2.

mutant synapses also had no impact on EPSC amplitude or quantal content (Fig. 4 *E–H*). However, in elevated extracellular Ca^{2+}, *DKaiR1D* has no apparent functions in basal neurotransmission nor in PHP expression (17), properties we confirmed were also shared by *dSol-1* (*SI Appendix*, Fig. S2). Together, these results are consistent with a model in which dSol-1 and DKaiR1D function together to promote baseline neurotransmitter release.

***DKaiR1D* Is Required for *dSol-1* to Potentiate Neurotransmitter Release.** There is precedent for enhanced expression of auxiliary GluR subunits to alter the synaptic delivery, abundance, stabilization, and/or activity of associated receptors. For example, increased TARP expression enhances AMPA receptor number, distribution, and gating in the hippocampus (43, 44), while muscle overexpression of *Drosophila neto-β* reduces postsynaptic GluR levels at the NMJ (34). Similarly, overexpression of *Sol-1* increases glutamate-gated currents through functional modulation of associated GluRs in *C. elegans* (41). Given that loss of *dSol-1* diminishes presynaptic glutamate release, we next asked whether elevated expression of *dSol-1* in motor neurons is sufficient to promote neurotransmitter release. Overexpression of *dSol-1* (dSol-1-OE) using a motor neuron-specific driver in an otherwise wild-type background potentiated baseline synaptic strength through an increase in EPSC amplitude, without significantly changing mEPSC amplitude (Fig. 5 *A–C* and *SI Appendix*, Table S2). Correspondingly, quantal content was increased by over 50% compared with baseline values (Fig. 5*D*), demonstrating that enhanced neuronal expression of *dSol-1* is sufficient to potentiate glutamate release from motor neurons.

Since *dSol-1* and *DKaiR1D* function in the same genetic pathway to promote release, we considered whether dSol-1-OE–mediated enhancement in release requires *DKaiR1D*. In moderate extracellular Ca^{2+} conditions, loss or overexpression of *DKaiR1D* has no impact on baseline synaptic transmission (Fig. 5 *A–D*) (17). However, overexpression of *dSol-1* in *DKaiR1D* mutant backgrounds failed to potentiate release (Fig. 5 *A–D*). Thus, increased *dSol-1* expression in neurons can potentiate transmitter release, but this ability requires *DKaiR1D*.

In principle, overexpression of *dSol-1* could increase the abundance and/or gating properties of DKaiR1D receptors to promote neurotransmitter release. However, in *C. elegans*, Sol-1 functions to modify the gating properties of GLR1, slowing desensitization and promoting open states, without having any apparent roles in modifying the abundance of surface GLR1 receptors at synapses or in heterologous cells (31, 41, 42). To gain insight into how overexpression of *dSol-1* potentiates release

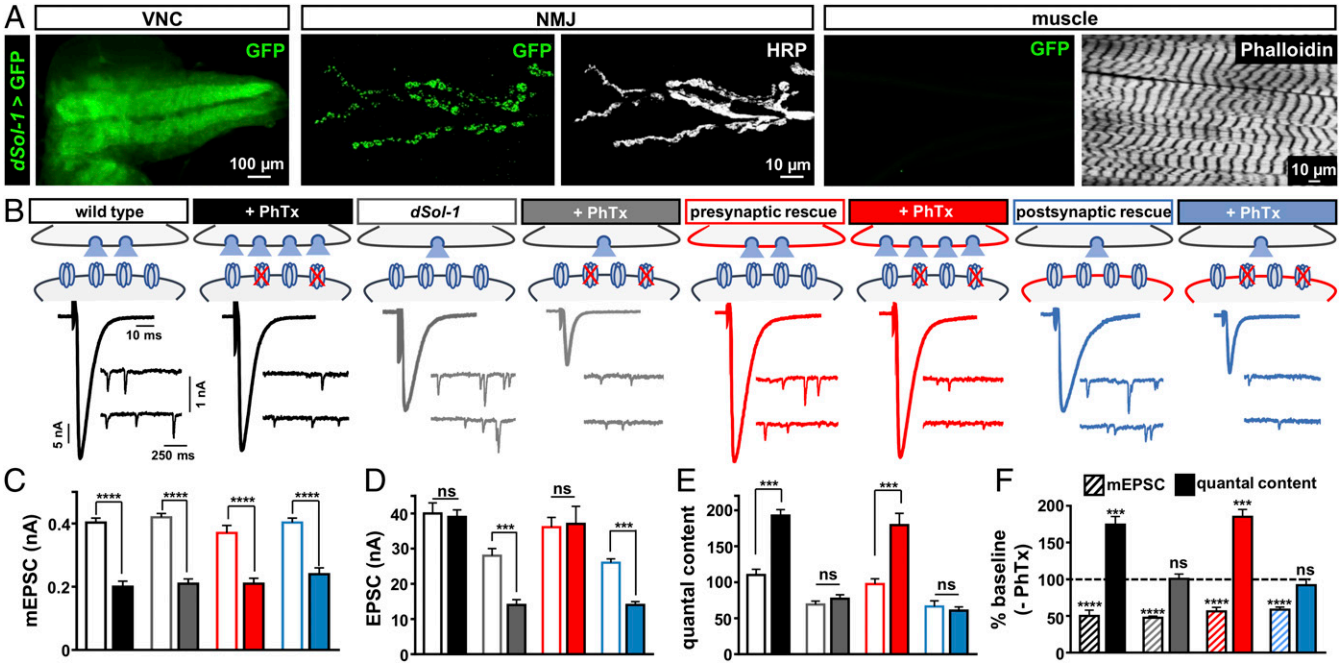

Fig. 3. Presynaptic *dSol-1* expression is necessary to promote basal neurotransmitter release and homeostatic potentiation. (*A*) Representative larval ventral nerve cord (VNC) and NMJ images of GFP expression driven by the *dSol-1* promoter and amplified with a Gal4-inducible *tubulin-Gal4* cassette (*w;dSol-1-Gal4/Tub-FRT-STOP-FRT-Gal4,UAS-FLP,UAS-CD8-GFP*). Anti-HRP (neuronal membrane marker) and anti-phalloidin (muscle actin marker) are shown. *dSol-1* is exclusively expressed in the nervous system with no detectible signal in the muscle. (*B*) Rapid expression of PHP requires *dSol-1*. Representative EPSC and mEPSC traces for wild type, *dSol-1*^{bk1} mutants, presynaptic rescue (neuronal expression of *dSol-1* in *dSol-1* mutants; *w;OK6-Gal4/UAS-dSol-1;dSol-1*^{bk1}), or postsynaptic rescue (muscle expression of *dSol-1* in *dSol-1* mutants; *w;G14-Gal4/UAS-dSol-1;dSol-1*^{bk1}) at baseline and after PhTx application. Presynaptic expression of *dSol-1* fully restores PHP expression, while PHP fails in the postsynaptic rescue condition. (*C–E*) Quantification of mEPSC amplitude (*C*), EPSC amplitude (*D*), and quantal content (*E*) values at baseline and after PhTx treatment. (*F*) Quantification of mEPSC amplitude and quantal content values following PhTx application relative to baseline (−PhTx) in the indicated genotypes. Error bars indicate ±SEM. ***$P < 0.001$, ****$P < 0.0001$; ns, not significant. Absolute values for normalized data are summarized in *SI Appendix*, Table S2.

in a *DKaiR1D*-dependent way, we immunostained synapses with an antibody against DKaiR1D at wild-type and dSol-1-OE NMJs. Overexpression of *DKaiR1D* in motor neurons (MN>DKaiR1D) is necessary for anti-DKaiR1D antibodies to reliably detect these receptors at NMJ terminals (17). MN>DKaiR1D does not significantly impact neurotransmission compared with wild type (Fig. 5 *A–D*), and we observed anti-DKaiR1D puncta that colocalized with the active zone marker *bruchpilot* (BRP), as has been previously shown (*Experimental Procedures* and Fig. 5*E*) (17). Interestingly, when both *DKaiR1D* and *dSol-1* were overexpressed together, release was potentiated to levels similar to dSol-1-OE alone (Fig. 5 *A–D*), but no increase in DKaiR1D punctum intensity, density, or localization relative to active zones was observed (Fig. 5 *E–H*). Although the mechanism through which dSol-1-OE potentiates neurotransmitter release is uncertain, these findings are consistent with overexpression of *dSol-1* potentiating presynaptic release through functional changes to existing DKaiR1D receptors, without apparent alterations to DKaiR1D receptor abundance or localization at individual release sites. Such a mechanism would parallel the means through which *C. elegans* Sol-1 modulates synaptic strength (41, 42).

***dSol-1* Promotes the Rapid Accumulation of DKaiR1D Receptors near Release Sites during PHP Signaling.** Neuronal overexpression of *dSol-1* potentiates neurotransmitter release to levels similar in magnitude to what is observed during PHP. One possibility is that dSol-1-OE promotes presynaptic release through a common mechanism shared with the adaptations that occur during PHP. Alternatively, dSol-1-OE may enhance release through a novel mechanism, distinct from the signaling that happens during PHP. In this case, increased quantal content induced by PHP expression would be expected to be additive with dSol-1-OE. We sought to distinguish between these possibilities by assessing PHP expression at dSol-1-OE NMJs. PhTx application to wild-type and dSol-1-OE NMJs reduced mEPSC amplitudes, as expected (Fig. 6 *A* and *B* and *SI Appendix*, Table S2). However, while wild-type EPSCs recovered to baseline levels after PhTx, EPSC values were correspondingly reduced in dSol-1-OE, failing to return to baseline levels (Fig. 6 *A* and *B* and *SI Appendix*, Table S2). This demonstrates that dSol-1-OE occludes additional PHP signaling, perhaps because PHP has effectively already been triggered.

Auxiliary subunits can function to increase the surface expression and synaptic localization of their respective GluRs (7, 9, 35, 45). In addition, auxiliary subunits can also affect the kinetics and gating properties of GluRs to modulate their activity (42, 43, 46). These mechanisms are not mutually exclusive. Neuronal overexpression of *dSol-1* potentiates neurotransmitter release through *DKaiR1D* without measurably changing receptor levels at presynaptic terminals (Fig. 5). In our final set of experiments, we sought to test whether PHP signaling modulates DKaiR1D receptor levels, and how *dSol-1* functions in this process.

We quantified DKaiR1D receptor puncta by immunostaining transgenically overexpressed *DKaiR1D* in controls and in *dSol-1* mutant backgrounds before and after PhTx application. In baseline conditions, relatively low levels of DKaiR1D puncta colocalized with BRP puncta, as observed previously (Fig. 5*E*) (17). Remarkably, after a 10-min incubation in PhTx, we found a substantial increase in DKaiR1D signals, including in the intensity and density of individual DKaiR1D puncta (Fig. 6 *C–E*), with a significant increase in the number of DKaiR1D puncta colocalized with BRP puncta at active zones (Fig. 6*F*).

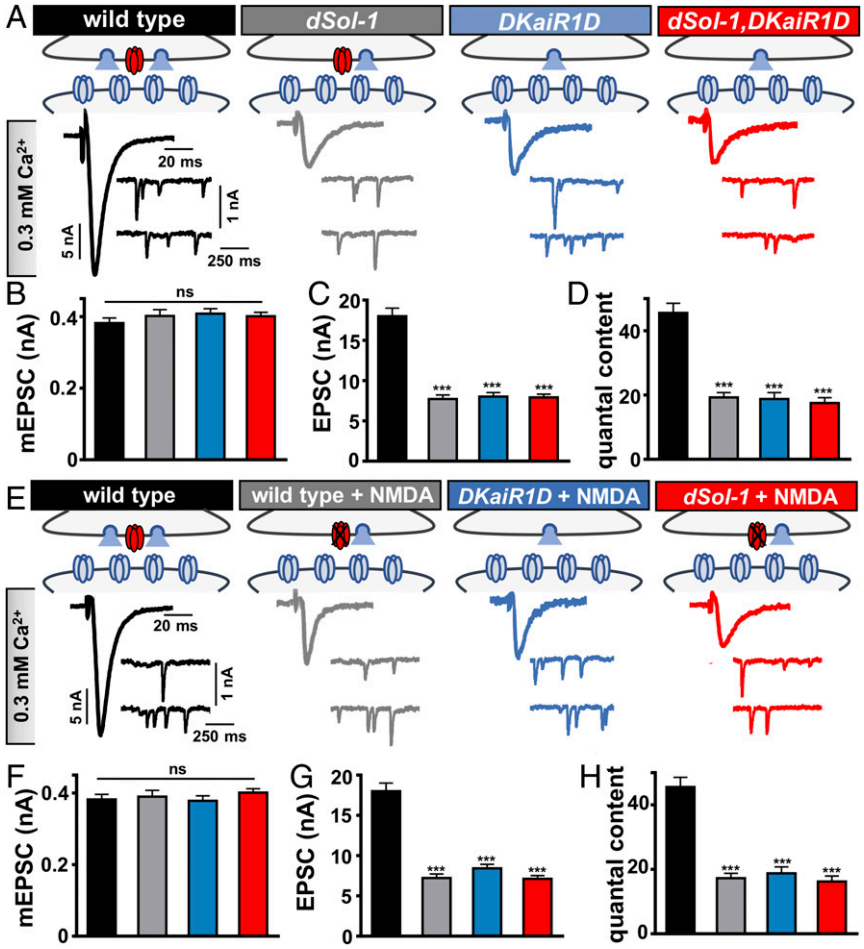

Fig. 4. *dSol-1* and *DKaiR1D* act in the same genetic pathway to promote baseline neurotransmitter release. (*A*) Schematics and representative electrophysiological recordings at 0.3 mM extracellular Ca^{2+} in wild type, *dSol-1* mutants (w;*dSol-1*^{bk1}), *DKaiR1D* mutants (*w;DKaiR1D*^{2}), and *dSol-1,DKaiR1D* double mutants (*w;dSol-1*^{bk1}*,DKaiR1D*^{2}). Note that the EPSC amplitude is not further reduced in *dSol-1,DKaiR1D* double mutants compared with either mutant alone. (*B–D*) Quantification of mEPSC amplitude (*B*), EPSC amplitude (*C*), and quantal content (*D*) values in the indicated genotypes. (*E*) Schematics and representative traces recorded in the presence of the DKaiR1D antagonist NMDA in 0.3 mM extracellular Ca^{2+} in the indicated genotypes. Application of NMDA to wild-type NMJs reduces baseline transmission but has no effect on *DKaiR1D* and *dSol-1* mutants. (*F–H*) Quantification of mEPSC amplitude (*F*), EPSC amplitude (*G*), and quantal content (*H*) values in the indicated genotypes and conditions. Error bars indicate ±SEM. ***$P < 0.001$; ns, not significant. Absolute values for normalized data are summarized in *SI Appendix*, Table S2.

Importantly, no increase in DKaiR1D levels was observed following PhTx application in *dSol-1* mutants (Fig. 6 *C–F*), indicating that *dSol-1* is required to rapidly enhance DKaiR1D receptors at presynaptic terminals during PHP signaling. Thus, *dSol-1* has two separable functions in promoting neurotransmitter release through DKaiR1D receptors. First, increased *dSol-1* expression enhances baseline neurotransmitter release without impacting DKaiR1D levels. However, *dSol-1* has an additional function during PHP signaling to promote the rapid accumulation of DKaiR1D receptors at presynaptic release sites.

Discussion

We have identified an auxiliary GluR subunit that functions in motor neurons to promote glutamate release during both baseline activity and homeostatic plasticity at the *Drosophila* NMJ. Genetic, pharmacological, and cell biological evidence suggests *dSol-1* functions with *DKaiR1D* to enhance neurotransmitter release. In the context of baseline neurotransmission, *dSol-1* promotes release without measurably changing the abundance or localization of DKaiR1D receptors, indicating a functional role in modulating DKaiR1D activity. However, *dSol-1* is necessary during PHP signaling to drive a rapid increase in DKaiR1D receptor abundance at presynaptic terminals. These findings define a CUB domain auxiliary GluR subunit as a central target for the presynaptic modulation of synaptic efficacy and homeostatic plasticity.

Several lines of evidence suggest that *dSol-1* enhances baseline neurotransmitter release by targeting DKaiR1D receptor functionality. First, *dSol-1* promotes baseline neurotransmission in low extracellular Ca^{2+}, a function shared with *DKaiR1D* (17). In addition, neurotransmitter release is reduced in *dSol-1* mutants and enhanced by neuronal overexpression of *dSol-1*, indicating a capacity for *dSol-1* expression levels to bidirectionally tune release. However, this potentiation in baseline transmission occurs without a significant increase in DKaiR1D receptor abundance, at least when both *dSol-1* and *DKaiR1D* are overexpressed in motor neurons (Fig. 5), suggesting a change in DKaiR1D functionality. Interestingly, in *C. elegans*, Sol-1 regulates GLR1 functionality by modulating channel gating, promoting the open state, and slowing sensitization, without an apparent change in *glr1* expression (31, 41, 42). In heterologous cells, both Sol-1 and dSol-1 promote GLR1 function without altering expression levels (42). This indicates a potentially conserved function between *sol-1* and *dSol-1* to confer similar modulations to GluR functionality. In mammals, Neto auxiliary subunits selectively associate with

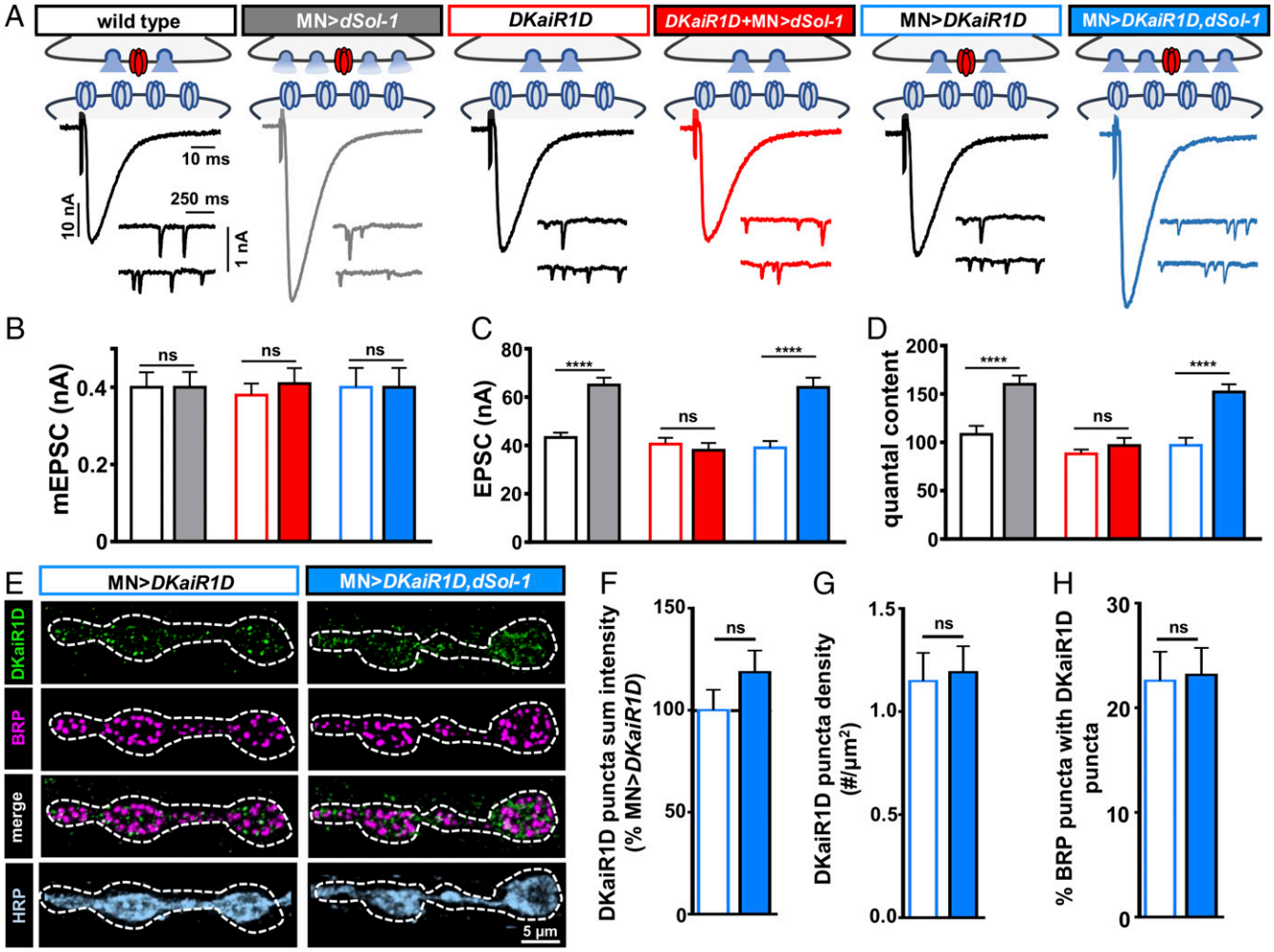

Fig. 5. DKaiR1D is required for *dSol-1* to potentiate baseline neurotransmitter release. (*A*) Schematics and representative EPSC and mEPSC traces showing *dSol-1* overexpression in motor neurons enhances presynaptic neurotransmitter release in wild type (MN>*dSol-1*: *w;OK6-Gal4/UAS-dSol-1*). However, *dSol-1* overexpression in motor neurons fails to increase presynaptic release in the absence of *DKaiR1D* (*DKaiR1D*+MN>*dSol-1*: *w;OK6-Gal4/UAS-dSol-1;DKaiR1D*^{2}). Overexpression of *DKaiR1D* at wild-type NMJs (MN>*DKaiR1D*: *w;OK6-Gal4/UAS-DKaiR1D*) does not impact neurotransmission and does not enhance release further in conjunction with *dSol-1* overexpression (MN>*DKaiR1D,dSol-1*: *w;UAS-dSol-1/UAS-DKaiR1D;D42-Gal4/+*). (*B–D*) Quantification of mEPSC amplitude (*B*), EPSC amplitude (*C*), and quantal content (*D*) values in the indicated genotypes. (*E*) Representative images of NMJs with *DKaiR1D* overexpressed in wild type (MN>*DKaiR1D*) or in combination with *dSol-1* (MN>*DKaiR1D,dSol-1*) immunostained with anti-DKaiR1D, -BRP, and -HRP. Note that no change in the DKaiR1D signal is observed in MN>*DKaiR1D,dSol-1* compared with MN>*DKaiR1D*. (*F–H*) Quantification of DKaiR1D punctum sum intensity (*F*), DKaiR1D punctum density (*G*) and percentage of BRP-positive active zones colocalized with DKaiR1D (*H*) reveals no significant change in MN>*DKaiR1D,dSol-1* compared with MN>*DKaiR1D*. Error bars indicate ±SEM. ****$P < 0.0001$; ns, not significant. Absolute values for normalized data are summarized in *SI Appendix*, Table S2.

kainate-subtype GluRs, while TARPs such as Stargazin associate with AMPA-type receptors (9, 29, 30). In *Drosophila*, Neto is an important auxiliary subunit for the postsynaptic GluRs at the NMJ, which, like DKaiR1D, are generally characterized as non-NMDA, kainate-type GluRs (28, 47, 48). However, in *C. elegans*, both Sol-1 and Sol-2/Neto form a complex together with the AMPA receptor subtype GLR1 (33), suggesting some level of promiscuity, at least in invertebrates, between AMPA and kainate GluRs and their auxiliary subunits. One possibility is that at baseline states, a substantial proportion of DKaiR1D receptors do not interact with dSol-1. By increasing levels of *dSol-1*, more DKaiR1D receptors may become associated with dSol-1, perhaps leading to changes in gating properties that enhance DKaiR1D receptor function. However, we cannot rule out the possibility that *dSol-1* somehow regulates *DKaiR1D* through a more indirect mechanism. While DKaiR1D receptors can form homomers and traffic to the cell surface when expressed alone in heterologous cells (28), future in vitro studies will be needed to determine the precise role dSol-1 has in DKaiR1D receptor trafficking and/or functionality.

dSol-1 enables PHP expression through a mechanism that is distinct from its role in baseline transmission, although both functions converge on *DKaiR1D*. Our data suggest that PHP signaling leads to a rapid accumulation of DKaiR1D receptors near presynaptic release sites that requires *dSol-1*. This *dSol-1*–dependent increase in DKaiR1D levels may be a unique feature of homeostatic signaling in *Drosophila*, as there is no evidence for worm *sol-1* to promote surface levels or changes in GLR1 localization in vivo or in vitro (31, 41, 42). Although the rapid increase in DKaiR1D receptor levels at synaptic terminals during PHP signaling is surprising, it is not unprecedented. DKaiR1D receptors are present near presynaptic release sites (17), and many other active zone components rapidly accumulate and/or remodel following PhTx application (49–54). An attractive

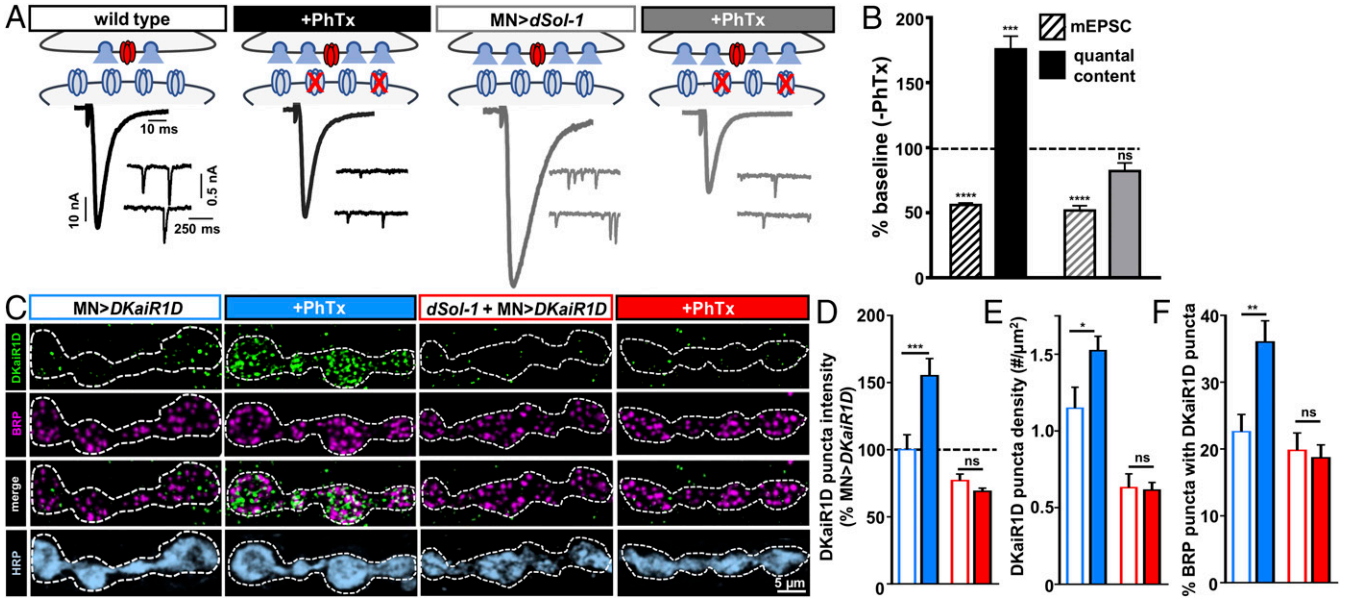

Fig. 6. PHP signaling requires *dSol-1* to promote rapid accumulation of DKaiR1D receptors near release sites. (*A*) Schematics and representative traces in the indicated genotypes showing presynaptic neurotransmitter release is not further enhanced following PhTx application at NMJs overexpressing *dSol-1* in motor neurons. (*B*) Quantification of mEPSC and quantal content values following PhTx application normalized to baseline (−PhTx) demonstrates quantal content is not further increased following PhTx application to MN>*dSol-1* NMJs. (*C*) Representative images of boutons immunostained with anti-DKaiR1D, -BRP, and -HRP at NMJs with *DKaiR1D* overexpressed in wild type (MN>*DKaiR1D*: *w;OK6-Gal4/UAS-DKaiR1D*) or *dSol-1* mutants (*dSol-1*+MN>*DKaiR1D*: *w;OK6-Gal4,dSol-1^{bk1}/UAS-DKaiR1D,dSol-1^{bk1}*) at baseline and following PhTx application. Note the increase in *DKaiR1D* signal after PhTx observed in wild type is not found in *dSol-1* mutants. (*D–F*) Quantification of DKaiR1D punctum sum intensity (*D*) and density (*E*) and percentage of BRP-positive active zones colocalized with DKaiR1D (*F*) reveals increases in MN>DKaiR1D following PhTx application, while no enhancement is observed in *dSol-1* mutants. Error bars indicate ±SEM. **P* < 0.05, ***P* < 0.01, ****P* < 0.001; ns, not significant. Absolute values for normalized data are summarized in *SI Appendix*, Table S2.

possibility is that DKaiR1D receptors participate in this process of rapid active zone remodeling during PHP signaling. Mechanistically, new protein synthesis of *DKaiR1D* is unlikely to be involved, as PHP expression (51, 55) and active zone remodeling (49) can occur without new translation. Recently, the lysosomal kinesin adaptor *arl-8* and other axonal transport factors were identified to be necessary for the rapid increase in active zone components during PHP signaling (49, 50). Thus, it is tempting to speculate that DKaiR1D receptors might be cotransported during PHP as part of this pathway. In vertebrates, auxiliary subunits traffic GluRs during synaptic plasticity (1, 45, 56), so dSol-1 may function similarly in delivering DKaiR1D receptors to the plasma membrane and/or to release sites during PHP signaling. Finally, it is possible that DKaiR1D receptors are constitutively degraded under baseline conditions, and that PHP signaling through *dSol-1* inhibits this degradation. The role of protein degradation in PHP signaling has been recently studied in both pre- and postsynaptic compartments at the *Drosophila* NMJ (57, 58). Interestingly, inhibition of proteasomal degradation in presynaptic compartments is capable of rapidly enhancing neurotransmission (58) to levels similar to what is observed after overexpression of *dSol-1*. In both cases, no further increase in neurotransmitter release is observed after PhTx application. While there are apparently distinct roles for *dSol-1* in baseline function and homeostatic plasticity, a common point of convergence is DKaiR1D.

CUB domains define a structural motif in a large family of extracellular and plasma membrane-associated proteins present in invertebrates to humans (59). While the specific four extracellular CUB domains that define *sol-1*/*dSol-1* are unique to invertebrates, genes containing multiple CUB domains (between two and eight) are present throughout vertebrate species and function in diverse processes including intercellular signaling, developmental patterning, inflammation, and tumor suppression (60, 61). CUB domains mediate dimerization and binding to collagen-like regions; this interaction may be relevant to its role in promoting PHP, as the *Drosophila* collagen member Multiplexin is present in the extracellular matrix and has been proposed to be part of the homeostatic retrograde signaling system (57, 62). Our characterization of *dSol-1* contrasts with what is known about another CUB domain auxiliary glutamate receptor in *Drosophila*, Neto-β. *neto-β* is highly expressed in the larval muscle, where it is clearly involved in the trafficking and/or stabilization of postsynaptic GluRs at the NMJ (34, 47). In contrast, *dSol-1* is exclusively expressed in the nervous system. Another interesting distinction is that while both dSol-1 and Neto contain multiple extracellular CUB domains and a single transmembrane domain, dSol-1 lacks any intracellular domain while two isoforms of Neto are expressed with one of two alternative intracellular C-terminal cytosolic domains, Neto-α or Neto-β (37). Neto-β is clearly the major isoform and performs the key functions in controlling postsynaptic GluR levels and composition (37), while *neto*-α was recently proposed to function in motor neurons with *DKaiR1D* and to be necessary for PHP (63). Interestingly, the *C. elegans* receptor GLR1 requires the auxiliary subunits Sol-1, Stargazin, and Neto/Sol-2 for functionality in vivo and in vitro (33, 42). It is therefore possible that *Drosophila* Neto-α and/or Stargazin-like interact with both dSol-1 and DKaiR1D. In mammals, there is a large body of evidence demonstrating that presynaptic GluRs, including kainate receptors, modulate presynaptic function (29). While postsynaptic kainate receptors in mammals associate with the CUB domain auxiliary GluR subunit Neto2 to regulate synaptic function and homeostatic plasticity (6, 33), to what extent Neto2 or other auxiliary subunits function with presynaptic kainate receptors remains enigmatic (29, 64). Our study indicates that CUB domain proteins may be fundamental modulators of GluRs in synaptic function and plasticity on both sides of the synapse.

Experimental Procedures

Fly Stocks. All *Drosophila* stocks were raised at 25 °C on standard molasses food. The w^{1118} strain was used as the wild-type control unless otherwise noted because this is the genetic background in which all genotypes are bred. Details of all stocks and their sources are listed in *SI Appendix*, Tables S1 and S3.

Molecular Biology. *dSol-1*^{bk1} and *dSol-1*^{bk2} mutants were generated using a CRISPR-Cas9 genome-editing strategy as described (65). Briefly, a target Cas9 cleavage site was selected early in the first coding exon of the *dSol-1* ORF without containing obvious off-target sequences in the *Drosophila* genome (sgRNA sequence: 5′-CTTGGCTCTGGGATTAACCGTGG-3′; protospacer-adjacent motif (PAM) sequence: underlined; off targets: 0; strand: +). This construct was sent to BestGene, Inc. for targeted insertion into the VK18 attP site on the second chromosome (66). Flies with the corresponding sgRNA sequences were crossed to a *vas-Cas9* line on the second chromosome to induce active germline CRISPR mutagenesis and 10 lines were screened for mutations. We found 4 lines that exhibited no mutations in the *dSol-1* locus (including *dSol-1*^{silent}) and identified 6 independent indels in the *dSol-1* gene. The two lines that were predicted to induce the earliest stop codons (L23STOP and Q41STOP) were chosen for further analysis and named *dSol-1*^{bk1} and *dSol-1*^{bk2}, respectively. To control for possible off-target lesions due to CRISPR-Cas9 mutagenesis, we also characterized a *dSol-1*^{silent} allele, which was derived from a chromosome that underwent the same Cas9 and sgRNA crosses that were used to generate the *dSol-1* mutant alleles but did not mutate the *dSol-1* locus.

To generate a *UAS-dSol-1* transgene, we obtained an expressed sequence tag (EST) (IP10972) encoding the entire *dSol-1* ORF from the Berkeley *Drosophila* Genome Project (https://www.fruitfly.org). We inserted the *dSol-1* complementary DNA into the pACU2 vector (67) using standard approaches. To generate the *dSol-1>Gal4* promotor fusion, we PCR-amplified a 4-kb region upstream of the *dSol-1* start codon and cloned this product into the pDEST-APIGH Gal4 expression vector using the Gateway expression system (Invitrogen). All constructs were sequenced to confirm fidelity and orientation and were sent to BestGene, Inc. for targeted insertion into the VK18 attP site on the second chromosome.

Immunochemistry. Third-instar larvae were dissected in ice-cold 0 Ca^{2+} HL-3 solution and immunostained as described (68, 69). Briefly, larvae were fixed in either Bouin's fixative (Sigma; HT10132-1L) or 4% paraformaldehyde in phosphate-buffered saline (PBS) (Sigma; F8775). Larvae were washed with PBS containing 0.1% Triton X-100 (PBST) for 30 min and blocked for 1 h in 5% normal donkey serum followed by overnight incubation in primary antibodies at 4 °C, washing in PBST, incubation in secondary antibodies for 2 h, washing again in PBST, and equilibration in 70% glycerol in PBST. Samples were mounted in VectaShield (Vector Laboratories). Details of all antibodies, their source, dilution, and references are listed in *SI Appendix*, Table S3.

Confocal Imaging and Analysis. Samples were imaged using a Nikon A1R resonant scanning confocal microscope equipped with NIS Elements software and a 100× APO 1.4 numerical aperture (NA) oil-immersion objective using separate channels with laser lines 488, 561, and 637 nm as described (70). *Z* stacks were obtained using identical settings for all genotypes, with *z*-axis spacing between 0.15 and 0.5 μm within an experiment and optimized for detection without saturation of the signal. Fluorescence-intensity measurements were taken on muscles 6/7 and muscle 4 of segment A3 for at least 10 NMJs acquired from at least 6 different animals. For fluorescence quantifications of the GluR subunits, the general analysis toolkit in the NIS Elements software was used as the binary for GluRIIA to measure values in GluRIIB and GluRIID channels. To measure synaptic growth, both type Ib and Is boutons were counted using vGlut-, horseradish peroxidase (HRP)-, and Dlg-stained NMJ terminals on muscles 6/7 and muscle 4 of segment A3, considering each vGlut punctum to be a bouton. The general analysis toolkit in the NIS Elements software was used to quantify BRP punctum number per NMJ and density was quantified by dividing the BRP punctum number by the neuronal membrane area masked by the HRP channel. For analysis of DKaiR1D puncta, BRP and DKaiR1D puncta were counted within an area also labeled by HRP and controls were performed to establish and subtract background levels of nonspecific signals due to the anti-rat secondary antibody used. To determine colocalization of DKaiR1D and BRP puncta, a binary mask was created for BRP puncta and only the DKaiR1D signal within that mask was quantified. BRP and DKaiR1D intensities were normalized to the HRP signal intensity and then normalized to wild-type values. Punctum density and intensity measurements based on confocal images were taken from at least 12 synapses acquired from at least 6 different animals.

Electrophysiology. Electrophysiological recordings were performed from muscle 6 in abdominal segments 2 and 3 from wandering third-instar larvae at room temperature as described (71, 72). Recordings were made in modified hemolymph-like saline (HL-3) containing 70 mM NaCl, 5 mM KCl, 10 mM $MgCl_2$, 10 mM $NaHCO_3$, 115 mM sucrose, 5 mM trehalose, 5 Hepes, and 0.5 $CaCl_2$ (unless specified) (pH 7.2) from cells with an initial V_m between −60 and −75 mV and input resistances >6 MΩ. Sharp intracellular electrodes with resistances of 12 to 25 MΩ filled with 3 M KCl were used. Recordings were performed with an Olympus BX61WI microscope using a 40×/0.80 NA water-dipping objective and acquired using an Axoclamp 900A amplifier, Digidata 1440A acquisition system, and pClamp 10.5 software (Molecular Devices). Electrophysiological sweeps were digitized at 10 kHz with a 1-kHz filter. For all TEVC recordings, muscles were clamped at −70 mV with a leak current below 10 nA and a settling time of the voltage clamp of 22.3 ms. For recordings at or above 1 mM Ca^{2+}, evoked EPSCs were recorded with a combination of HS-9Ax10 and HS-9Ax1 head stages (Axon CNS; Molecular Devices). For recordings at <1 mM Ca^{2+}, two HS-9Ax1 head stages were used. From each muscle cell, 100 mEPSCs were recorded in the absence of stimulation. Twenty EPSCs were acquired for each cell under stimulation at 0.5 Hz and stimulus duration of 0.5 ms, and with stimulus intensity adjusted with an ISO-Flex Stimulus Isolator (A.M.P.I.). Quantal content was calculated by dividing the average EPSC amplitude by the average mEPSC amplitude for each cell. To acutely block postsynaptic receptors, larvae were incubated with or without philanthotoxin-433 (20 μM; Sigma) in HL-3 for 10 min as described (55). For the acute blockade of DKaiR1D by NMDA, larvae were dissected and, following a 10-min incubation with PhTx, the central nervous system was removed and the larvae were incubated with 1 mM NMDA (Abcam; ab120052; resuspended in deionized H_2O) for 5 min, with recordings performed in the continued presence of NMDA as described (17). Data were analyzed using Clampfit 10.7 (Molecular Devices), MiniAnalysis (Synaptosoft), Excel (Microsoft), and Prism (GraphPad Software).

Statistical Analysis. Data were analyzed using GraphPad Prism (version 7.0) or Microsoft Excel software (version 16.22). Datasets were tested for normality using the D'Agostino and Pearson omnibus test to ensure that the assumption of normality was not violated. Values were then compared using either a one-way ANOVA, followed by Tukey's multiple-comparison test, or an unpaired two-tailed Student's *t* test with Welch's correction. All data are presented as mean ± SEM; *P* denotes the level of significance assessed (*$P < 0.05$, **$P < 0.01$, ***$P < 0.001$, ****$P < 0.0001$; ns, not significant). Statistics of all experiments are summarized in *SI Appendix*, Table S2.

Data Availability. All study data are included in the article and *SI Appendix*.

ACKNOWLEDGMENTS. We acknowledge the Developmental Studies Hybridoma Bank (Iowa) for antibodies and the Bloomington *Drosophila* Stock Center for fly stocks (NIH Grant P40OD018537). This work was supported by a grant from the NIH (NS091546) (to D.D.).

1. G. H. Diering, R. L. Huganir, The AMPA receptor code of synaptic plasticity. *Neuron* **100**, 314–329 (2018).
2. B. E. Herring, R. A. Nicoll, Long-term potentiation: From CaMKII to AMPA receptor trafficking. *Annu. Rev. Physiol.* **78**, 351–365 (2016).
3. V. A. Derkach, M. C. Oh, E. S. Guire, T. R. Soderling, Regulatory mechanisms of AMPA receptors in synaptic plasticity. *Nat. Rev. Neurosci.* **8**, 101–113 (2007).
4. I. Pérez-Otaño, M. D. Ehlers, Homeostatic plasticity and NMDA receptor trafficking. *Trends Neurosci.* **28**, 229–238 (2005).
5. D. Chowdhury, J. W. Hell, Homeostatic synaptic scaling: Molecular regulators of synaptic AMPA-type glutamate receptors. *F1000 Res.* **7**, 234 (2018).
6. W. Zhang *et al.*, A transmembrane accessory subunit that modulates kainate-type glutamate receptors. *Neuron* **61**, 385–396 (2009).
7. D. Bissen, F. Foss, A. Acker-Palmer, AMPA receptors and their minions: Auxiliary proteins in AMPA receptor trafficking. *Cell. Mol. Life Sci.* **76**, 2133–2169 (2019).
8. S. Tomita, Regulation of ionotropic glutamate receptors by their auxiliary subunits. *Physiology* **25**, 41–49 (2010).
9. A. C. Jackson, R. A. Nicoll, The expanding social network of ionotropic glutamate receptors: TARPs and other transmembrane auxiliary subunits. *Neuron* **70**, 178–199 (2011).
10. P. S. Pinheiro *et al.*, GluR7 is an essential subunit of presynaptic kainate autoreceptors at hippocampal mossy fiber synapses. *Proc. Natl. Acad. Sci. U.S.A.* **104**, 12181–12186 (2007).
11. D. Schmitz, J. Mellor, M. Frerking, R. A. Nicoll, Presynaptic kainate receptors at hippocampal mossy fiber synapses. *Proc. Natl. Acad. Sci. U.S.A.* **98**, 11003–11008 (2001).

12. R. Scott, T. Lalic, D. M. Kullmann, M. Capogna, D. A. Rusakov, Target-cell specificity of kainate autoreceptor and Ca^{2+}-store-dependent short-term plasticity at hippocampal mossy fiber synapses. *J. Neurosci.* **28**, 13139–13149 (2008).
13. A. Banerjee, R. S. Larsen, B. D. Philpot, O. Paulsen, Roles of presynaptic NMDA receptors in neurotransmission and plasticity. *Trends Neurosci.* **39**, 26–39 (2016).
14. L. Bogdanik *et al*., The *Drosophila* metabotropic glutamate receptor DmGluRA regulates activity-dependent synaptic facilitation and fine synaptic morphology. *J. Neurosci.* **24**, 9105–9116 (2004).
15. A. Pittaluga, Presynaptic release-regulating mGlu1 receptors in central nervous system. *Front. Pharmacol.* **7**, 295 (2016).
16. C. Upreti, X. L. Zhang, S. Alford, P. K. Stanton, Role of presynaptic metabotropic glutamate receptors in the induction of long-term synaptic plasticity of vesicular release. *Neuropharmacology* **66**, 31–39 (2013).
17. B. Kiragasi, J. Wondolowski, Y. Li, D. K. Dickman, A presynaptic glutamate receptor subunit confers robustness to neurotransmission and homeostatic potentiation. *Cell Rep.* **19**, 2694–2706 (2017).
18. S. Takayanagi-Kiya, K. Zhou, Y. Jin, Release-dependent feedback inhibition by a presynaptically localized ligand-gated anion channel. *eLife* **5**, e21734 (2016).
19. G. W. Davis, M. Müller, Homeostatic control of presynaptic neurotransmitter release. *Annu. Rev. Physiol.* **77**, 251–270 (2015).
20. C. A. Frank, T. D. James, M. Müller, Homeostatic control of *Drosophila* neuromuscular junction function. *Synapse* **74**, e22133 (2020).
21. C. A. Frank, Homeostatic plasticity at the *Drosophila* neuromuscular junction. *Neuropharmacology* **78**, 63–74 (2014).
22. X. Wang, J. M. McIntosh, M. M. Rich, Muscle nicotinic acetylcholine receptors may mediate trans-synaptic signaling at the mouse neuromuscular junction. *J. Neurosci.* **38**, 1725–1736 (2018).
23. X. Wang, M. J. Pinter, M. M. Rich, Reversible recruitment of a homeostatic reserve pool of synaptic vesicles underlies rapid homeostatic plasticity of quantal content. *J. Neurosci.* **36**, 828–836 (2016).
24. B. O. Orr *et al*., Presynaptic homeostasis opposes disease progression in mouse models of ALS-like degeneration: Evidence for homeostatic neuroprotection. *Neuron* **107**, 95–111.e6 (2020).
25. S. G. Cull-Candy, R. Miledi, A. Trautmann, O. D. Uchitel, On the release of transmitter at normal, myasthenia gravis and myasthenic syndrome affected human end-plates. *J. Physiol.* **299**, 621–638 (1980).
26. X. Wang, M. M. Rich, Homeostatic synaptic plasticity at the neuromuscular junction in myasthenia gravis. *Ann. N. Y. Acad. Sci.* **1412**, 170–177 (2018).
27. I. Delvendahl, K. Kita, M. Müller, Rapid and sustained homeostatic control of presynaptic exocytosis at a central synapse. *Proc. Natl. Acad. Sci. U.S.A.* **116**, 23783–23789 (2019).
28. Y. Li *et al*., Novel functional properties of *Drosophila* CNS glutamate receptors. *Neuron* **92**, 1036–1048 (2016).
29. J. Lerma, J. M. Marques, Kainate receptors in health and disease. *Neuron* **80**, 292–311 (2013).
30. R. A. Nicoll, S. Tomita, D. S. Bredt, Auxiliary subunits assist AMPA-type glutamate receptors. *Science* **311**, 1253–1256 (2006).
31. Y. Zheng, J. E. Mellem, P. J. Brockie, D. M. Madsen, A. V. Maricq, SOL-1 is a CUB-domain protein required for GLR-1 glutamate receptor function in *C. elegans*. *Nature* **427**, 451–457 (2004).
32. D. Ng *et al*., Neto1 is a novel CUB-domain NMDA receptor-interacting protein required for synaptic plasticity and learning. *PLoS Biol.* **7**, e41 (2009).
33. R. Wang *et al*., The SOL-2/Neto auxiliary protein modulates the function of AMPA-subtype ionotropic glutamate receptors. *Neuron* **75**, 838–850 (2012).
34. Y. J. Kim, H. Bao, L. Bonanno, B. Zhang, M. Serpe, *Drosophila* Neto is essential for clustering glutamate receptors at the neuromuscular junction. *Genes Dev.* **26**, 974–987 (2012).
35. B. A. Copits, G. T. Swanson, Dancing partners at the synapse: Auxiliary subunits that shape kainate receptor function. *Nat. Rev. Neurosci.* **13**, 675–686 (2012).
36. C. Straub, S. Tomita, The regulation of glutamate receptor trafficking and function by TARPs and other transmembrane auxiliary subunits. *Curr. Opin. Neurobiol.* **22**, 488–495 (2012).
37. C. I. Ramos, O. Igiesuorobo, Q. Wang, M. Serpe, Neto-mediated intracellular interactions shape postsynaptic composition at the *Drosophila* neuromuscular junction. *PLoS Genet.* **11**, e1005191 (2015).
38. K. Chen, C. Merino, S. J. Sigrist, D. E. Featherstone, The 4.1 protein coracle mediates subunit-selective anchoring of *Drosophila* glutamate receptors to the postsynaptic actin cytoskeleton. *J. Neurosci.* **25**, 6667–6675 (2005).
39. M. Wang *et al*., Dbo/Henji modulates synaptic dPAK to gate glutamate receptor abundance and postsynaptic response. *PLoS Genet.* **12**, e1006362 (2016).
40. E. Metwally, G. Zhao, W. Li, Q. Wang, Y. Q. Zhang, Calcium-activated calpain specifically cleaves glutamate receptor IIA but not IIB at the *Drosophila* neuromuscular junction. *J. Neurosci.* **39**, 2776–2791 (2019).
41. Y. Zheng *et al*., SOL-1 is an auxiliary subunit that modulates the gating of GLR-1 glutamate receptors in *Caenorhabditis elegans*. *Proc. Natl. Acad. Sci. U.S.A.* **103**, 1100–1105 (2006).
42. C. S. Walker *et al*., Conserved SOL-1 proteins regulate ionotropic glutamate receptor desensitization. *Proc. Natl. Acad. Sci. U.S.A.* **103**, 10787–10792 (2006).
43. A. D. Milstein, W. Zhou, S. Karimzadegan, D. S. Bredt, R. A. Nicoll, TARP subtypes differentially and dose-dependently control synaptic AMPA receptor gating. *Neuron* **55**, 905–918 (2007).
44. N. Rouach *et al*., TARP gamma-8 controls hippocampal AMPA receptor number, distribution and synaptic plasticity. *Nat. Neurosci.* **8**, 1525–1533 (2005).
45. R. L. Huganir, R. A. Nicoll, AMPARs and synaptic plasticity: The last 25 years. *Neuron* **80**, 704–717 (2013).
46. N. Sheng, Y. S. Shi, R. M. Lomash, K. W. Roche, R. A. Nicoll, Neto auxiliary proteins control both the trafficking and biophysical properties of the kainate receptor GluK1. *eLife* **4**, e11682 (2015).
47. T. H. Han, P. Dharkar, M. L. Mayer, M. Serpe, Functional reconstitution of *Drosophila melanogaster* NMJ glutamate receptors. *Proc. Natl. Acad. Sci. U.S.A.* **112**, 6182–6187 (2015).
48. A. Schmid *et al*., Non-NMDA-type glutamate receptors are essential for maturation but not for initial assembly of synapses at *Drosophila* neuromuscular junctions. *J. Neurosci.* **26**, 11267–11277 (2006).
49. M. A. Böhme *et al*., Rapid active zone remodeling consolidates presynaptic potentiation. *Nat. Commun.* **10**, 1085 (2019).
50. P. Goel *et al*., Homeostatic scaling of active zone scaffolds maintains global synaptic strength. *J. Cell Biol.* **218**, 1706–1724 (2019).
51. P. Goel, X. Li, D. Dickman, Disparate postsynaptic induction mechanisms ultimately converge to drive the retrograde enhancement of presynaptic efficacy. *Cell Rep.* **21**, 2339–2347 (2017).
52. S. J. Gratz *et al*., Endogenous tagging reveals differential regulation of Ca^{2+} channels at single active zones during presynaptic homeostatic potentiation and depression. *J. Neurosci.* **39**, 2416–2429 (2019).
53. A. Weyhersmüller, S. Hallermann, N. Wagner, J. Eilers, Rapid active zone remodeling during synaptic plasticity. *J. Neurosci.* **31**, 6041–6052 (2011).
54. A. Mrestani *et al*., Active zone compaction in presynaptic homeostatic potentiation. bioRxiv:10.1101/802843 (22 May 2020).
55. C. A. Frank, M. J. Kennedy, C. P. Goold, K. W. Marek, G. W. Davis, Mechanisms underlying the rapid induction and sustained expression of synaptic homeostasis. *Neuron* **52**, 663–677 (2006).
56. A. C. Jackson, R. A. Nicoll, Stargazin (TARP γ-2) is required for compartment-specific AMPA receptor trafficking and synaptic plasticity in cerebellar stellate cells. *J. Neurosci.* **31**, 3939–3952 (2011).
57. K. Kikuma *et al*., Cul3 and insomniac are required for rapid ubiquitination of postsynaptic targets and retrograde homeostatic signaling. *Nat. Commun.* **10**, 2998 (2019).
58. C. Wentzel, I. Delvendahl, S. Sydlik, O. Georgiev, M. Müller, Dysbindin links presynaptic proteasome function to homeostatic recruitment of low release probability vesicles. *Nat. Commun.* **9**, 267 (2018).
59. P. Bork, G. Beckmann, The CUB domain. A widespread module in developmentally regulated proteins. *J. Mol. Biol.* **231**, 539–545 (1993).
60. G. Blanc *et al*., Insights into how CUB domains can exert specific functions while sharing a common fold: Conserved and specific features of the CUB1 domain contribute to the molecular basis of procollagen C-proteinase enhancer-1 activity. *J. Biol. Chem.* **282**, 16924–16933 (2007).
61. C. Gaboriaud *et al*., Structure and properties of the Ca(2+)-binding CUB domain, a widespread ligand-recognition unit involved in major biological functions. *Biochem. J.* **439**, 185–193 (2011).
62. T. Wang, A. G. Hauswirth, A. Tong, D. K. Dickman, G. W. Davis, Endostatin is a trans-synaptic signal for homeostatic synaptic plasticity. *Neuron* **83**, 616–629 (2014).
63. T. H. Han *et al*., Neto-α controls synapse organization and homeostasis at the *Drosophila* neuromuscular junction. *Cell Rep.* **32**, 107866 (2020).
64. M. S. Wyeth *et al*., Neto auxiliary subunits regulate interneuron somatodendritic and presynaptic kainate receptors to control network inhibition. *Cell Rep.* **20**, 2156–2168 (2017).
65. K. Kikuma, X. Li, D. Kim, D. Sutter, D. K. Dickman, Extended synaptotagmin localizes to presynaptic ER and promotes neurotransmission and synaptic growth in *Drosophila*. *Genetics* **207**, 993–1006 (2017).
66. K. J. Venken, Y. He, R. A. Hoskins, H. J. Bellen, P[acman]: A BAC transgenic platform for targeted insertion of large DNA fragments in *D. melanogaster*. *Science* **314**, 1747–1751 (2006).
67. C. Han, L. Y. Jan, Y. N. Jan, Enhancer-driven membrane markers for analysis of non-autonomous mechanisms reveal neuron-glia interactions in *Drosophila*. *Proc. Natl. Acad. Sci. U.S.A.* **108**, 9673–9678 (2011).
68. S. Perry, Y. Han, A. Das, D. Dickman, Homeostatic plasticity can be induced and expressed to restore synaptic strength at neuromuscular junctions undergoing ALS-related degeneration. *Hum. Mol. Genet.* **26**, 4153–4167 (2017).
69. S. Perry *et al*., Developmental arrest of *Drosophila* larvae elicits presynaptic depression and enables prolonged studies of neurodegeneration. *Development* **147**, dev186312 (2020).
70. P. Goel *et al*., A screen for synaptic growth mutants reveals mechanisms that stabilize synaptic strength. *J. Neurosci.* **39**, 4051–4065 (2019).
71. P. Goel, X. Li, D. Dickman, Estimation of the readily releasable synaptic vesicle pool at the *Drosophila* larval neuromuscular junction. *Bio. Protoc.* **9**, e3127 (2019).
72. X. Chen *et al*., The BLOC-1 subunit pallidin facilitates activity-dependent synaptic vesicle recycling. *eNeuro* **4**, 1–18 (2017).